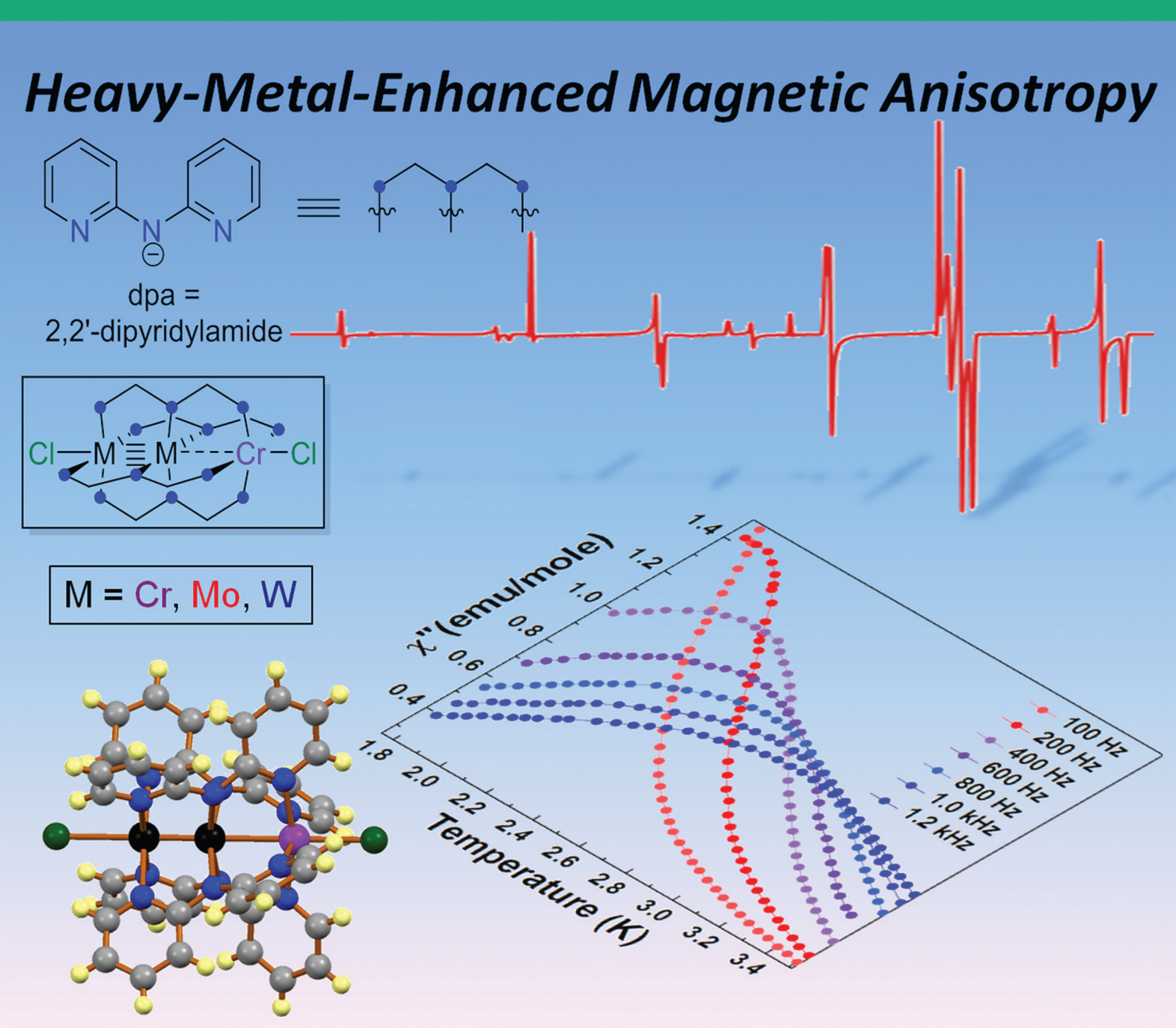
# 1019anic Chemistry July 4, 2016

July 4, 2016 Volume 55, Number 13 pubs.acs.org/IC



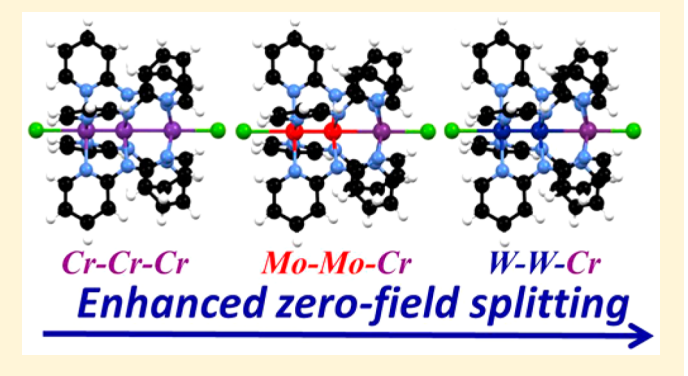




# Enhancing the Magnetic Anisotropy of Linear Cr(II) Chain Compounds Using Heavy Metal Substitutions

Jonathan H. Christian, David W. Brogden, Jasleen K. Bindra, Jared S. Kinyon, Johan van Tol, Jingfang Wang, John F. Berry, and Naresh S. Dalal.

**ABSTRACT:** Magnetic properties of the series of three linear, trimetallic chain compounds  $Cr_2Cr(dpa)_4Cl_2$ , **1**,  $Mo_2Cr(dpa)_4Cl_2$ , **2**, and  $W_2Cr(dpa)_4Cl_2$ , **3** (dpa=2,2'-dipyridylamido), have been studied using variable-temperature dc and ac magnetometry and high-frequency EPR spectroscopy. All three compounds possess an S=2 electronic ground state arising from the terminal  $Cr^{2+}$  ion, which exhibits slow magnetic relaxation under an applied magnetic field, as evidenced by ac magnetic susceptibility and magnetization measurements. The slow relaxation stems from the existence of an easy-axis magnetic anisotropy, which is bolstered by the axial symmetry of the compounds and has been quantified through rigorous high-frequency EPR measurements. The magnitude of D in



these compounds increases when heavier ions are substituted into the trimetallic chain; thus D = -1.640, -2.187, and -3.617 cm<sup>-1</sup> for  $Cr_2Cr(dpa)_4Cl_2$ ,  $Mo_2Cr(dpa)_4Cl_2$ , and  $W_2Cr(dpa)_4Cl_2$ , respectively. Additionally, the D value measured for  $W_2Cr(dpa)_4Cl_2$  is the largest yet reported for a high-spin  $Cr^{2+}$  system. While earlier studies have demonstrated that ligands containing heavy atoms can enhance magnetic anisotropy, this is the first report of this phenomenon using heavy metal atoms as "ligands".

# ■ INTRODUCTION

Multimetallic coordination compounds featuring a linear array of metals are of considerable current interest due to their interesting structural and physical properties. One of the most prominent classes of such compounds are linear, trimetallic species supported by the 2,2'-dipyridylamide (dpa) ligand, shown in Chart 1. A broad suite of homometallic  $M_3(dpa)_4Cl_2$  (M=Cr, Co, Ni, Cu, Ru, Rh) and heterometallic  $M_2M'(dpa)_4Cl_2$  compounds (M=Cr, Mo, W, Ru; M'=typically a first-row transition metal element) have been

Chart 1

dpa = 2,2'-dipyridylamide

1: 
$$M = Cr$$
2:  $M = Mo$ 
3:  $M = W$ 

extensively explored,<sup>3</sup> and a number of them display fascinating magnetic properties. For example,  $\text{Co}_3(\text{dpa})_4\text{Cl}_2$  compounds show spin equilibrium behavior between their S=1/2 ground states and a high-spin (S=3/2 or 5/2) excited state.<sup>5–12</sup> In the heterometallic  $\text{M}_2\text{Co}(\text{dpa})_4\text{Cl}_2$ , when M=Cr, the  $S=1/2 \rightleftharpoons S=3/2$  spin equilibrium behavior is retained, but  $\text{Mo}_2\text{Co}(\text{dpa})_4\text{Cl}_2$  is high-spin at all temperatures.<sup>13</sup> Thus, the properties of heterometallic chain compounds can be similar to or different from their homometallic analogues.

Chain compounds containing Cr(II) also display interesting magnetic properties. For example, even though  $Cr_3(dpa)_4Cl_2$  and related compounds can show either symmetric Cr-Cr-Cr or asymmetric  $Cr\equiv Cr\cdots Cr$  structures, they always display a well-isolated S=2 magnetic state. For the parent compound,  $Cr_3(dpa)_4Cl_2$ , 1, a 15 K crystal structure indicates a symmetric structure, but at higher temperatures the structure is asymmetric. Thus, the S=2 state for the compound is most easily rationalized as stemming from the presence of an "isolated" Cr(II) ion in the structure, with the  $Cr\equiv Cr$ 

Received: November 4, 2015 Published: February 16, 2016

<sup>&</sup>lt;sup>†</sup>Department of Chemistry and Biochemistry, Florida State University, Tallahassee, Florida 32306, United States

<sup>&</sup>lt;sup>‡</sup>Department of Chemistry, University of Wisconsin – Madison, 1101 University Avenue Madison, Wisconsin 53706, United States <sup>§</sup>National High Magnetic Field Laboratory, Florida State University, 1800 East Paul Dirac Drive, Tallahassee, Florida 32306, United

Supporting Information

quadruply bonded unit essentially remaining diamagnetic. The actual electronic structure, as probed by DFT methods, is a bit more nuanced. <sup>18–23</sup> Although orbitals of  $\pi$  and  $\delta$  symmetry for the "isolated" Cr(II) ion may be considered to be localized, its  $\sigma$ -symmetry  $d_{z2}$  orbital engages in bonding with the  $Cr \equiv Cr$  unit, yielding a three-center/three-electron  $\sigma$  bond such that the unpaired electron in the  $\sigma$ -symmetry orbital is delocalized among all three metal atoms as well as the axial ligands.

The Dalal group has longstanding interest in the magnetic properties of Cr compounds, <sup>24–32</sup> as well as metal–metal bonded chain compounds. <sup>33–35</sup> In general, there have been a relatively small number of studies of the magnetic properties of Cr<sup>2+</sup> complexes, likely due to their tendency for oxidation to  $\operatorname{Cr}^{3+}$ ,  $\operatorname{^{36}}$  and the zero-field splitting (zfs) parameter D has been determined in very few cases.  $\operatorname{^{37-43}}$  Nevertheless, this ion has often been shown to possess an easy-axis anisotropy (D < 0), $^{37-40,43-46}$  which is helpful for developing compounds that exhibit slow magnetic relaxation in zero applied field.<sup>47–50</sup> Because of their ease of synthesis<sup>51</sup> and tunable properties,<sup>14</sup> Cr(II) chain compounds attracted our attention as a potential novel class of single-molecule magnets. We therefore investigated compound 1 using high-frequency EPR spectroscopy to determine the sign and magnitude of D; we recently reported that 1 has D = -1.6 cm<sup>-1</sup> and therefore predicted that it should show magnetic blocking behavior. 52 More recently, magnetic blocking in a related penta-chromium chain has been reported by Cornia and co-workers.<sup>53</sup>

Here, we present a full report of the single-molecule magnet properties of 1, as well as two heterometallic analogues,  $Mo_2Cr(dpa)_4Cl_2$  (2) and  $W_2Cr(dpa)_4Cl_2$  (3), the preparation of which we recently reported. This series (Chart 1) is studied to test the hypothesis that substitution of the  $Cr \equiv Cr$  unit in 1 with the heavier  $Mo \equiv Mo$  or  $W \equiv W$  group would enhance the magnetic anisotropy of the Cr(II) ion via the increased spin—orbit coupling of the heavy metal atoms. The "heavy ion effect" has been used previously as a design principle for single-molecule magnets by use of heavy halogen or chalcogen ligands,  $^{41,54-58}_{}$  as well as incorporation of paramagnetic metals into polyoxotungstates. This is the first example of a direct metal—metal bond being used to transmit the heavy ion effect, where we may consider the  $Cr_2$ ,  $Mo_2$ , or  $W_2$  units as "ligands" to the Cr(II) ion.

# EXPERIMENTAL SECTION

Magnetic Susceptibility Measurements. Compounds 1-3 were prepared using published methods. 18,51 Polycrystalline samples were weighed and placed inside of borosilicate glass tubes, which were sealed under a vacuum to avoid air exposure during measurements. Variable-temperature dc magnetic susceptibility was measured using a Quantum Design MPMS-XL SQUID magnetometer over a temperature range of 1.8-300 K at a measuring field of 0.02 T. The data were fit using the julX magnetic simulation program. <sup>59</sup> Variable-temperature ac magnetic susceptibility was also measured between 1.8 and 4.0 K and frequencies from 100 Hz to 1.2 kHz. Because of the need for higher frequencies (vide infra), variable-temperature, variablefrequency ac magnetic susceptibilities of 2 and 3 were measured using a Quantum Design PPMS over a temperature range of 1.8-6.0 K, and frequencies from 1 to 10 kHz. All ac susceptibility data were collected under 0 and 0.2 T dc magnetic fields. Hysteresis measurements were made with a sweep rate of 0.2 T min<sup>-1</sup>. Diamagnetic corrections for each sample were calculated using Pascal constants<sup>60</sup> and were applied to the experimental data along with a contribution from the sample holder.

EPR Measurements. High-field/high-frequency (240 GHz) EPR measurements were conducted at the National High Magnetic Field

Laboratory (NHMFL) in Tallahassee, FL, over the temperature range from 300 to 4 K and fields up to 12 T using a laboratory developed Superheterodyne high-frequency EPR spectrometer. The instrument consists of an Oxford Instruments superconducting magnet, a 15 GHz Gunn diode with frequency doublers, a multifrequency wave bridge, a sample probe with a corrugated waveguide, Schottky diode detectors, low-noise amplifiers, 6 GHz mixers, lock-in amplifiers for phase sensitive detection, a magnetic field modulator, and a temperature control system. <sup>61,62</sup> The magnetic field was calibrated using a DPPH standard (g = 2.0036). <sup>63</sup> The spectra were simulated using the locally developed SPIN computer program, which diagonalizes the spin Hamiltonian matrix. <sup>42,64</sup>

#### RESULTS AND DISCUSSION

**Structural Features of 1–3.** Compounds 1–3 contain Cr(II) ions in nearly identical coordination environments. Furthermore, **2** and **3** crystallize isomorphously in the same space group (C2/c), and therefore differences in crystal packing effects are negligible. While the crystal packing environment of **1** is different (Pnn2), and intermolecular distances between Cr(II) centers in all three structures are >8.0 Å and are not expected to give rise to any of the magnetic properties we observe. The Cr–N bond distances for all three compounds fall within the very small range of 2.12–2.13 Å, and the Cr–Cl distances range from 2.53–2.54 Å. The major structural differences in the direct coordination sphere involve the heterometallic Cr–M distances, which are 2.48, 2.69, and 2.65 Å, for **1**, **2**, and **3**, respectively.

**Magnetic Measurements.** Variable-temperature magnetic susceptibility measurements of 1–3 are shown in Figure 1. The compounds have effective magnetic moments at room temperature of 4.95  $\mu_{\rm B}$ , 4.78  $\mu_{\rm B}$ , and 4.88  $\mu_{\rm B}$ , respectively, which are all close to the spin-only value for an S=2 magnetic system ( $\mu_{\rm eff}=4.89~\mu_{\rm B}$  when g=2). Observation of an S=2 ground state is consistent with previous experimental studies,  $^{16,18,52}$  as well as previous electronic structure work on the compounds.  $^{18,23}$ 

The magnetic data were analyzed using the standard spin Hamiltonian, eq 1, with axial (D) and rhombic (E) zfs parameters.

$$\hat{H} = \beta \vec{H} \cdot \tilde{g} \cdot \hat{S} + D(\hat{S}_z^2 - \hat{S}^2/3) + E(\hat{S}_x^2 - \hat{S}_y^2)$$
(1)

Here,  $\beta$  is the Bohr magneton,  $\tilde{g}$  is the electronic Zeeman tensor, and the operators have their usual meanings. Because the effect of rhombicity on the magnetic susceptibility is small, E was not included in this model; however, it was used for EPR analysis (vide infra). The data in Figure 1 are well simulated using the parameters: S=2,  $g_{\text{average}}=2.014$ , and |D|=1.643 cm<sup>-1</sup> for 1; S=2,  $g_{\text{average}}=1.988$ , and |D|=2.187 cm<sup>-1</sup> for 2; and S=2,  $g_{\text{average}}=2.001$ , and |D|=3.617 cm<sup>-1</sup> for 3. The data can be fit using either positive or negative values for D; the negative values are given here as their modulus to indicate that the sign of D cannot be determined from this measurement alone. As anticipated from our "heavy metal effect" hypothesis, the magnitude of D increases as the Cr $\equiv$ Cr unit is changed to Mo $\equiv$ Mo and W $\equiv$ W. Although the dc magnetic data are not indicative of the sign of D, our previous results an engative D for 1 and therefore suggest that 2 and 3 might also have negative values of D.

The measurement of appreciable easy-axis zfs in the magnetic susceptibility, and the recent report of magnetic blocking in a pentachromium(II) chain complex,<sup>53</sup> provided us the impetus to measure variable-temperature ac magnetic susceptibility for

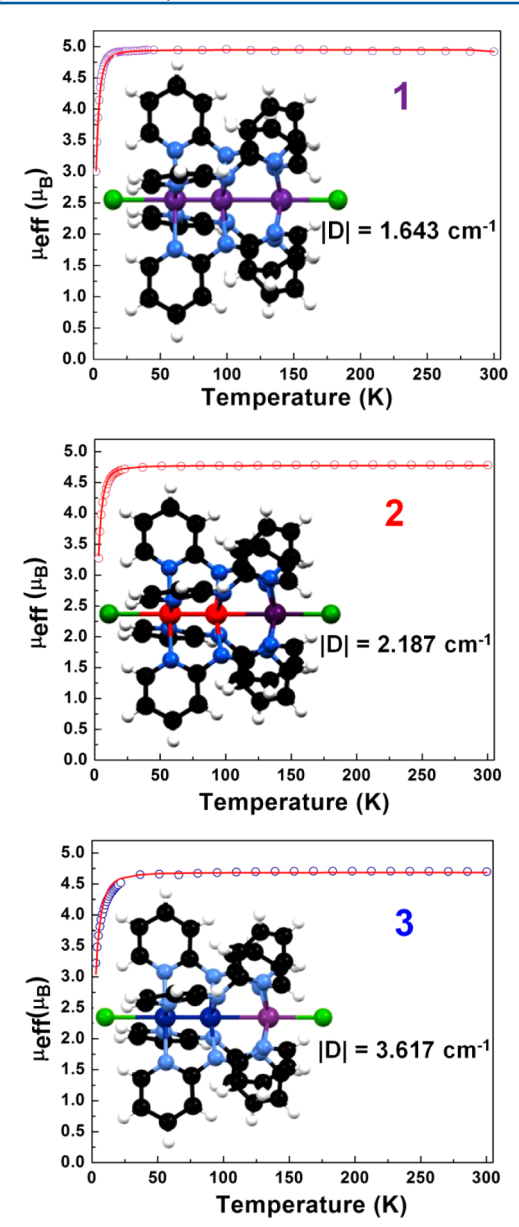


**Figure 1.** Variable-temperature molar magnetic susceptibility data for polycrystalline samples of 1 (top), 2 (middle), and 3 (bottom), collected at 0.02 T at temperatures from 1.8 to 300 K. The red line corresponds to a simulated set of susceptibility data using S=2 (see Table1 for exact g values), and negative values for D, as described in the text. The insets show a three-dimensional structure for each compound as well as the derived |D| values.

1–3. Measurements that were made without an applied magnetic field at frequencies between 100 Hz and 1.2 kHz all exhibited simple paramagnetic behavior. This was also the case for the pentrachromium(II) chain complexes where magnetic blocking was only observed under a 0.25 T dc field. Therefore, measurements on 1–3 were made using a dc field of 0.2 T. Under this field,  $\chi''$  became detectable for each compound, thus showing that the static field is effective in slowing the magnetic relaxation in these compounds.

The ac data for 1 are shown in Figure 2. Here, a clear frequency dependence in  $\chi''$  is observed, indicating slow magnetic relaxation consistent with single-molecule magnet behavior. In Figure 2,  $\ln(\tau)$  is plotted as a function of 1/T, where  $\tau = 1/(2 \pi \nu)$  and T is the temperature of the peak

position in  $\chi''$ . The Arrhenius plot is fairly linear ( $R^2 = 0.98$ ) over the measured temperature region, suggesting that magnetic relaxation in 1 proceeds via an Orbach process.<sup>47</sup> A linear fit of the data yields the energy barrier of spin relaxation  $(U_{\text{eff}})$  and the characteristic spin reversal time  $(\tau_0)$ , which are  $U_{\rm eff} = 7.4 \pm 0.4 \text{ cm}^{-1} \text{ and } \tau_0 = (2.9 \times 10^{-6}) \pm (0.5 \times 10^{-6}) \text{ s.}$ This value of  $U_{\rm eff}$  is in close agreement with the total splitting of the S = 2 multiplet calculated from the magnetic susceptibility and EPR-derived (vide infra) D ( $U = |D|S^2 = 6.56$  cm<sup>-1</sup>). We were struck to observe such a large value for  $\tau_0$ , because this parameter in SMMs is usually on the nanosecond time scale.  $^{66-70}$  However, the  $au_0$  value observed here is similar in magnitude to that measured for the pentachromium chain:  $2.2(5) \times 10^{-6}$  s.<sup>53</sup> This result may hint that the magnetic relaxation in 1 as well as its penta-chromium analogue does not approach a completely thermally activated relaxation over the measured temperature range.<sup>56</sup>

The ac magnetic susceptibilities of 2 and 3 were also measured in a dc field of 0.2 T (see Figures S1 and S2). Although an out-of-phase  $\chi''$  signal was measured for each compound, which indicates slow magnetic relaxation, the peaks were significantly broadened, and only a small frequency dependence in  $\chi''$  was observed. The frequency dependence was too small to yield a meaningful Arrhenius analysis.

Variable-temperature, variable-field magnetization measurements (Figure 3) revealed more information about the slow magnetic relaxation in these compounds. Specifically, each compound exhibits weak hysteretic behavior at low temperatures, but remnant magnetization at 0 field is absent, indicating that the magnetic relaxation in 1-3 is fast. For these compounds to exhibit remnant magnetization (i.e., the signature property of single-molecule magnets) requires lower temperatures or a faster field sweep than is achievable with our current instrumentation. Nevertheless, there is an important trend that we observe for these compounds regarding their hysteresis properties. The highest temperature at which hysteresis is observed is specific to each compound. Specifically, the hysteretic behavior ends at 10, 15, and 20 K (all  $\pm 4$  K), for 1, 2, and 3, respectively (see Figures S3-S5). This trend suggests that the energy barrier for spin relaxation in these compounds is largest for 3 and smallest for 1, a result that agrees with the determination of *D* from magnetic susceptibility measurements as well as our "heavy metal effect" hypothesis.

The results from magnetization measurements, showing that each compound exhibits different magnetic behavior based on the type of M<sup>II</sup> ions in the linear chain, called for further investigation by an independent technique. High-frequency and -field electron paramagnetic resonance (HFEPR) spectroscopy is arguably the best technique for studying the electronic states of a magnetic material at the molecular level; thus we initiated variable-temperature HFEPR to further elucidate the electronic structure of these compounds.

Well-resolved EPR spectra were observed for all three compounds at 240 GHz microwave frequency. To obtain the magnetic parameters of each compound, the spectra are analyzed according to eq 1 given above with S=2. Because no hyperfine splitting is apparent in the measured spectra, no hyperfine interactions are included in the spectral analysis. The best simulation models yielded the following parameters: for 1,  $g_x = 1.998$ ,  $g_y = 1.997$ ,  $g_z = 1.981$ , D = -1.643 cm<sup>-1</sup>, and E/D = 0.021; for 2,  $g_x = 1.960$ ,  $g_y = 1.960$ ,  $g_z = 1.991$ , D = -2.187 cm<sup>-1</sup>, and a small E/D = 0.011; for 3,  $g_x = 1.960$ ,  $g_y = 1.960$ ,  $g_z = 1.991$ , D = -3.617 cm<sup>-1</sup>, and E/D = 0.007. The experimental

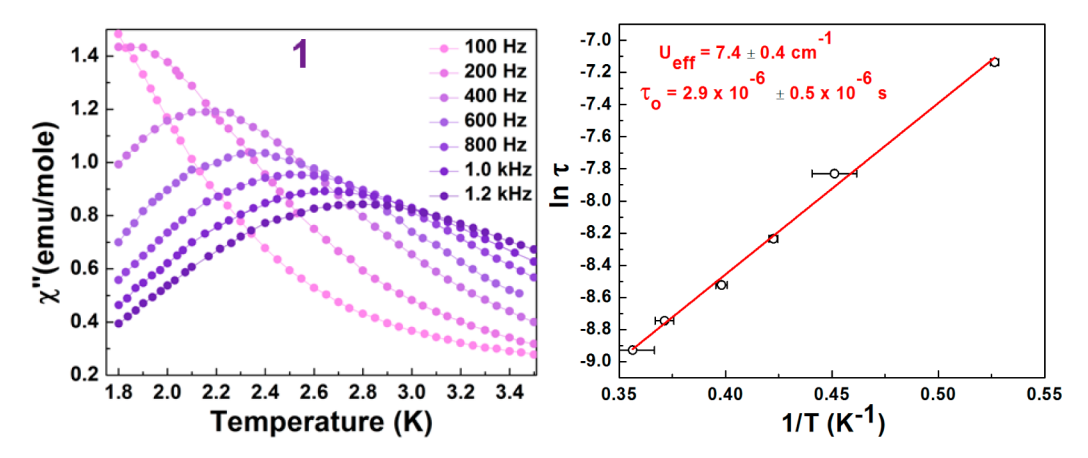


Figure 2. Left: Variable-temperature, variable-frequency ac magnetic susceptibility measurements of 1 under an applied dc field of 0.2 T. Right: Arrhenius plot of the relaxation rate versus inverse temperature for 1, with the linear fitting values given.

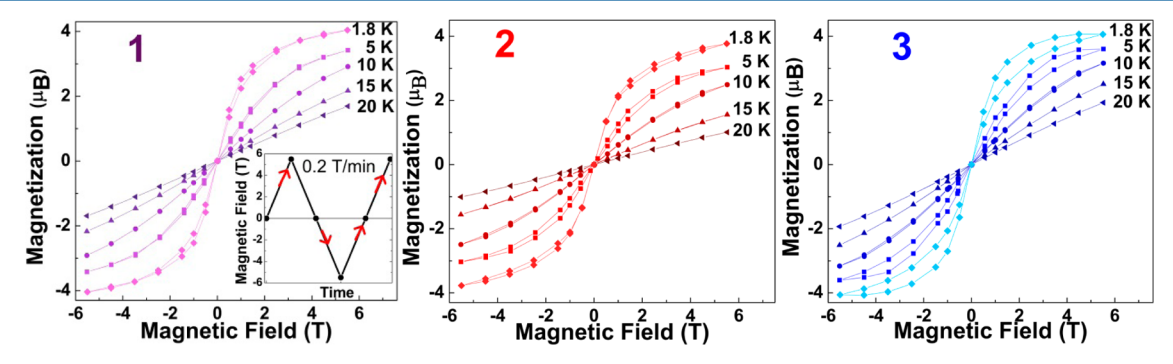


Figure 3. Variable-field magnetization data at 1.8, 5, 10, 15, and 20 K for 1 (left), 2 (center), and 3 (right). The inset (left) shows the sequence in which the magnetic field was swept at a rate of 0.2 T min<sup>-1</sup> during the magnetization measurements.

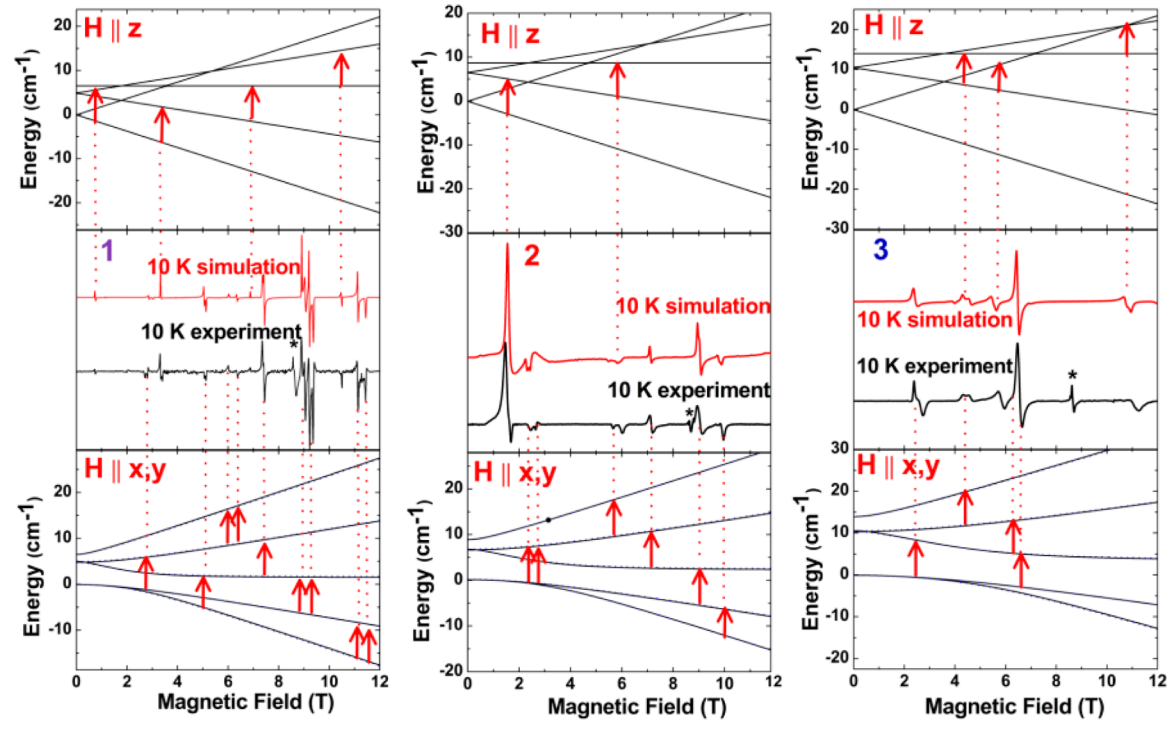


Figure 4. HFEPR (240 GHz, 10 K) spectra of 1 (left), 2 (center), and 3 (right). Both the experimental and the simulated spectra are shown along with the calculated energy level diagrams both parallel (top) and perpendicular (bottom) to the principal symmetry axis of the molecule. The red arrows mark the EPR transition assignments. The "\*" indicates a g = 2 impurity that was not simulated.

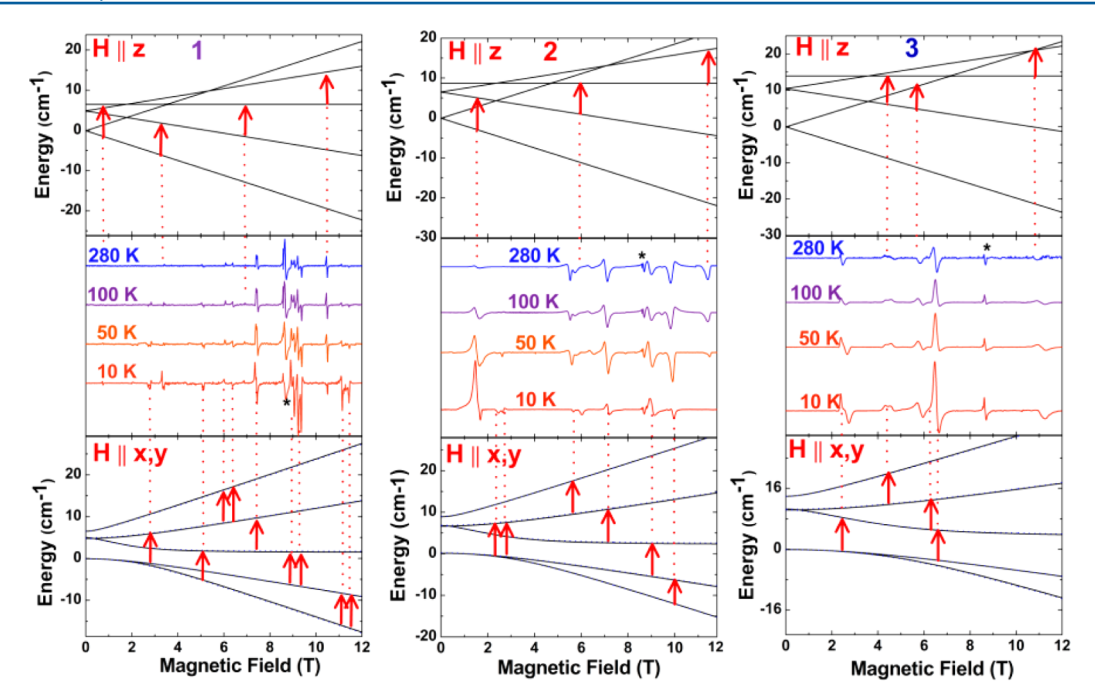


Figure 5. Variable-temperature 240 GHz EPR spectra of 1 (left), 2 (center), and 3 (right), measured between 280 and 10 K.

Table 1. Magnetic Parameters of 1-3

complex	S	$g_{\rm av}^{a}$	$g_x$	$g_y$	$g_z$	$D (cm^{-1})$	E/D	$\zeta (\text{cm}^{-1})^b$
1	2	2.014	1.998	1.997	1.981	-1.640	0.021	360
2	2	1.988	1.960	1.960	1.991	-2.187	0.011	420
3	2	2.001	1.980	1.980	2.110	-3.500	0.011	530

<sup>a</sup>The  $g_{av}$  values are those derived from magnetic susceptibility data. Otherwise, the data in this table are determined from EPR spectra. <sup>b</sup>The  $\zeta$  values are calculated effective spin—orbit coupling constants for the Cr<sup>II</sup> ions in the trimetallic chains (see eq 2).<sup>72,74</sup>

and simulated spectra are shown in Figure 4 along with the calculated energy level diagrams.

While the simulated spectra are in splendid agreement with the experimental data, confirmation of the sign of D is most accurately obtained through variable-temperature HFEPR, where Boltzmann population effects can be seen. 42,72,73 Although it is generally thought that low temperatures (liquid N<sub>2</sub> or even liquid He) are needed to observe EPR spectra of high-spin systems, we found this not to be the case for 1-3. Thus, 240 GHz EPR spectra were measured between 280 and 10 K. As shown in Figure 5, the most notable difference between the 280 and 10 K spectra of 1 is the increased intensity of the peaks at 3 T and above 11 T. According to the simulated energy level diagrams (Figure 5, top and bottom portions), these peaks correspond to transitions from the lowest energy states, which are the most populated states at low temperatures as shown in the Boltzmann distribution calculation for this compound (Figure S6). This observation confirms the assignment of a negative value of D for the compound. For 2 (Figure 5, middle), the significant increase in intensity of the peak at 1.7 T and the disappearance of the feature at 11.5 T upon cooling to 10 K also confirm the negative sign of D, because the low-field peak is attributed to a ground-state transition in the H||z| direction, while the disappearing highfield peak is attributed to an excited-state transition. Similar considerations for 3 reveal the negative D parameter, based on the ground-state transition at 6.7 T, which shows a marked increase in intensity upon cooling from 280 to 10 K.

Perhaps, the most remarkable aspect of these spectra and simulations is that each compound has strong easy-axis anisotropy, which increases in magnitude as the size of the  $M^{II}$  ions in the trinuclear chain increases. Thus, |D| (3) > |D| (2) > |D| (1). The underlying mechanism of this increase may be attributed to the spin—orbit parameter from the  $M^{II}$  ions because D is directly related to the spin—orbit coupling constant,  $\zeta$ . Abragam and Bleaney provide the following equations for a  $3d^4$  ion (here neglecting spin—spin coupling, with  $g_e$  being the free electron g value and  $\Delta$  being the octahedral ligand field splitting):

$$D = -\frac{3}{16} \frac{\zeta^2}{\Delta} \tag{2}$$

$$g_{\perp} = g_{\rm e} - \frac{1}{2} \frac{\zeta}{\Delta} \tag{3}$$

$$g_{\parallel} = g_{\rm e} - 2\frac{\zeta}{\Delta} \tag{4}$$

Though  $\Delta$  is not known for these complexes (the distortion from octahedral geometry is significant), we may make an estimate of 15 000 cm<sup>-1</sup>, somewhat larger than the 12 000–13 000 cm<sup>-1</sup> values determined for the Cr(II) aqua ion.<sup>39</sup> Assuming  $\Delta = 15\,000$  cm<sup>-1</sup>, the following  $\zeta$  values (representing effective free-ion spin–orbit coupling, reduced due to covalency) may be derived from eq 2:  $\zeta(1) = 360$  cm<sup>-1</sup>,  $\zeta(2) = 420$  cm<sup>-1</sup>, and  $\zeta(3) = 530$  cm<sup>-1</sup>. Thus, these data show an increase in effective spin–orbit coupling in this series from

Cr to Mo to W. However, we note that eqs 3 and 4 predict that  $g_{\parallel}$  must always be lower than  $g_{\perp}$ , in disagreement with our results for the Mo and W complexes. Nevertheless, the derived spin—orbit coupling constants are given in Table 1 along with other HFEPR-derived magnetic parameters.

To better visualize the increase of D as a function of the  $M^{II}$  ion size, we highlight the z-directed  $m_S = -2 \rightarrow m_S = -1$  and  $m_S = -1 \rightarrow m_S = 0$  transitions of each compound in Figure 6.

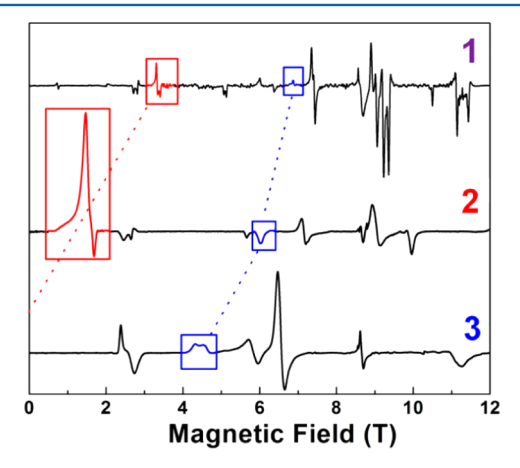


**Figure 6.** 10 K HFEPR spectra of 1, 2, and 3 are shown for direct comparison. Highlighted are the *z*-directed  $m_S = -2 \rightarrow m_S = -1$  (red) and  $m_S = -1 \rightarrow m_S = 0$  (blue) transitions, which shift to lower fields as the magnitude of *D* increases.

With a constant g-value, as is nearly the case here, these transitions are predicted to move to lower field positions with increasing D, and this is exactly what is observed. Another important feature that is clearly evident in Figure 6 is that the spectral line widths get noticeably broader with increasing  $M^{II}$  ion size. EPR line broadening is commonly caused by g-anisotropy due to the electrostatic field from neighboring molecules or D-strain from internal magnetic fields. Broadening due to D-strain may very well be the case here, because the broadening increases with the magnitude of D. However, we cannot rule out the possibility of broadening due to weak intermolecular exchange interactions that exist in these compounds, although this interpretation does not provide a useful explanation for why the magnitude of intermolecular exchange interactions might depend on the size of  $M^{II}$ .

# CONCLUSIONS

Trimetallic chain compounds 1, 2, and 3 have analogous magnetic properties stemming from their electronic structure containing a nearly isolated high-spin, S = 2 Cr(II) center. In an applied field, the Cr(II) ions show slow magnetic relaxation as a consequence of their highly axial magnetic anisotropy that is buttressed by the geometry of the metal-metal bond. The anisotropy, described quantitatively in the axial zfs term D, is enhanced in the series from 1 to 2 to 3, due to the "heavy-atom effect" of the M≣M group. This effect is clearly observed in variable-temperature high-field EPR spectra of the compounds, from which accurate determinations of D for the compounds have been made. The magnitude of the D value for 3, -3.617cm<sup>-1</sup>, is the largest yet reported for a high-spin Cr(II) compound, with the exception of chromocene, 46 which is an orbitally degenerate spin triplet and thus quite different from the octahedral high-spin Cr(II) complexes of interest here. This class of compounds shows promise for highly tunable magnetic properties. Further examples of these chain compounds are now being studied so that their full potential may be reached.

#### ASSOCIATED CONTENT

# **S** Supporting Information

The Supporting Information is available free of charge on the ACS Publications website at DOI: 10.1021/acs.inorg-chem.5b02545.

Variable-temperature, variable-frequency ac magnetic susceptibility measurements of 2 and 3, Arrhenius plot of the relaxation rate versus inverse temperature for 2 and 3, and a Boltzmann population calculation for 1 using the EPR-derived magnetic parameters (PDF)

# AUTHOR INFORMATION

# **Corresponding Authors**

\*E-mail: berry@chem.wisc.edu. \*E-mail: dalal@chem.fsu.edu.

#### Notes

The authors declare no competing financial interest.

# ACKNOWLEDGMENTS

We wish to acknowledge support from the National Science Foundation via grant CHE-1300464. J.H.C. and N.S.D. wish to thank Tiffany Christian for important assistance with magnetic measurements, and Naoki Kikugawa and Ryan Baumbach for useful discussions. We thank Dr. Andrew Ozarowski for giving us access to the SPIN program, and Dr. Eckhard Bill for giving us access to the julx program. We additionally thank Joshua Telser from Roosevelt University for contributing substantially to the discussion of spin—orbit coupling presented here. A portion of the work was performed at the national High Magnetic Field Laboratory, supported by the National Science Foundation (DMR-1157490) and the State of Florida.

# REFERENCES

- (1) Berry, J. F. In *Metal–Metal Bonding*; Parkin, G., Ed.; Springer: New York, 2010; Vol. 136, pp 1–28.
- (2) Berry, J. F. In *Multiple Bonds Between Metal Atoms*, 3rd ed.; Cotton, F. A., Murillo, C. A., Walton, R. A., Eds.; Springer Science and Business Media, Inc.: New York, 2005.
- (3) Brogden, D. W.; Berry, J. F. Comments Inorg. Chem. 2016, 36, 17-37.
- (4) Hua, S. A.; Cheng, M. C.; Chen, C. H.; Peng, S. M. Eur. J. Inorg. Chem. 2015, 2015, 2510–2523.
- (5) Berry, J. F.; Cotton, F. A.; Murillo, C. A.; Roberts, B. K. Inorg. Chem. 2004, 43, 2277–2283.
- (6) Berry, J. F.; Cotton, F. A.; Lu, T. B.; Murillo, C. A. Inorg. Chem. 2003, 42, 4425–4430.
- (7) Clérac, R.; Cotton, F. A.; Jeffery, S. P.; Murillo, C. A.; Wang, X. P. *Inorg. Chem.* **2001**, *40*, 1265–1270.
- (8) Clérac, R.; Cotton, F. A.; Daniels, L. M.; Dunbar, K. R.; Murillo, C. A.; Wang, X. P. J. Chem. Soc., Dalton Trans. 2001, 386–391.
- (9) Clérac, R.; Cotton, F. A.; Daniels, L. M.; Dunbar, K. R.; Murillo, C. A.; Wang, X. P. *Inorg. Chem.* **2001**, *40*, 1256–1264.
- (10) Clérac, R.; Cotton, F. A.; Daniels, L. M.; Dunbar, K. R.; Kirschbaum, K.; Murillo, C. A.; Pinkerton, A. A.; Schultz, A. J.; Wang, X. P. J. Am. Chem. Soc. 2000, 122, 6226–6236.
- (11) Clérac, R.; Cotton, F. A.; Dunbar, K. R.; Lu, T. B.; Murillo, C. A.; Wang, X. P. *Inorg. Chem.* **2000**, *39*, 3065–3070.
- (12) Cotton, F. A.; Murillo, C. A.; Wang, X. P. Inorg. Chem. 1999, 38, 6294-6297.
- (13) Nippe, M.; Victor, E.; Berry, J. F. Eur. J. Inorg. Chem. 2008, 2008, 5569-5572.

(14) Berry, J. F.; Cotton, F. A.; Lu, T. B.; Murillo, C. A.; Roberts, B. K.; Wang, X. P. J. Am. Chem. Soc. **2004**, 126, 7082–7096.

- (15) Cotton, F. A.; Lei, P.; Murillo, C. A. Inorg. Chim. Acta 2003, 349, 173–181.
- (16) Clérac, R.; Cotton, F. A.; Daniels, L. M.; Dunbar, K. R.; Murillo, C. A.; Pascual, I. *Inorg. Chem.* **2000**, *39*, 748–751.
- (17) Wu, L. C.; Thomsen, M. K.; Madsen, S. R.; Schmoekel, M.; Jorgensen, M. R. V.; Cheng, M. C.; Peng, S. M.; Chen, Y. S.; Overgaard, J.; Iversen, B. B. *Inorg. Chem.* **2014**, *53*, 12489–12498.
- (18) Brogden, D. W.; Christian, J. H.; Dalal, N. S.; Berry, J. F. *Inorg. Chim. Acta* **2015**, 424, 241–247.
- (19) Mohan, P. J.; Georgiev, V. P.; McGrady, J. E. Chem. Sci. 2012, 3, 1319-1329.
- (20) Georgiev, V. P.; McGrady, J. E. J. Am. Chem. Soc. 2011, 133, 12590-12599.
- (21) Rohmer, M. M.; Bénard, M. J. Cluster Sci. 2002, 13, 333-353.
- (22) Rohmer, M. M.; Bénard, M. Chem. Soc. Rev. 2001, 30, 340-354.
- (23) Benbellat, N.; Rohmer, M. M.; Bénard, M. Chem. Commun. 2001, 2368-2369.
- (24) Samuel, P. P.; Neufeld, R.; Mondal, K. C.; Roesky, H. W.; Herbst-Irmer, R.; Stalke, D.; Demeshko, S.; Meyer, F.; Rojisha, V. C.; De, S.; Parameswaran, P.; Stuckl, A. C.; Kaim, W.; Christian, J. H.; Bindra, J. K.; Dalal, N. S. *Chem. Sci.* **2015**, *6*, 3148–3153.
- (25) Liu, W. J.; Christian, J. H.; Al-Oweini, R.; Bassil, B. S.; van Tol, J.; Atanasov, M.; Neese, F.; Dalal, N. S.; Kortz, U. *Inorg. Chem.* **2014**, 53, 9274–9283.
- (26) Blinc, R.; Cevc, P.; Potocnik, A.; Zemva, B.; Goreshnik, E.; Hanzel, D.; Gregorovic, A.; Trontelj, Z.; Jaglicic, Z.; Laguta, V.; Perovic, M.; Dalal, N. S.; Scott, J. F. *J. Appl. Phys.* **2010**, *107*, 043511.
- (27) Nellutla, S.; Pati, M.; Jo, Y. J.; Zhou, H. D.; Moon, B. H.; Pajerowski, D. M.; Yoshida, Y.; Janik, J. A.; Balicas, L.; Lee, Y.; Meisel, M. W.; Takano, Y.; Wiebe, C. R.; Dalal, N. S. *Phys. Rev. B: Condens. Matter Mater. Phys.* **2010**, *81*, 064431.
- (28) Choi, K. Y.; Nellutla, S.; Reyes, A. P.; Kuhns, P. L.; Jo, Y. J.; Balicas, L.; Nojiri, H.; Pati, M.; Dalal, N. S. *Phys. Rev. B: Condens. Matter Mater. Phys.* **2008**, *78*, 214419.
- (29) Nellutla, Ś.; Choi, K. Y.; Pati, M.; van Tol, J.; Chiorescu, I.; Dalal, N. S. *Phys. Rev. Lett.* **2007**, *99*, 137601.
- (30) Harter, A.; Cage, B.; Nguyen, P.; Abboud, K. A.; Dalal, N. S. *Polyhedron* **2005**, *24*, 2350–2354.
- (31) Cotton, F. A.; Dalal, N. S.; Hillard, E. A.; Huang, P. L.; Murillo, C. A.; Ramsey, C. M. *Inorg. Chem.* **2003**, *42*, 1388–1390.
- (32) Ramsey, C. M.; Cage, B.; Nguyen, P.; Abboud, K. A.; Dalal, N. S. Chem. Mater. 2003, 15, 92–99.
- (33) Dalal, N. S.; Murillo, C. A. Dalton Trans. 2014, 43, 8565-8576.
- (34) Wang, J. F.; Ozarowski, A.; Kovnir, K.; Thompson, C. M.; Yaroslavtsev, A. A.; Chernikov, R. V.; Dalal, N. S.; Shatruk, M. Eur. J. Inorg. Chem. 2012, 2012, 4652–4660.
- (35) Nippe, M.; Wang, J. F.; Bill, E.; Hope, H.; Dalal, N. S.; Berry, J. F. J. Am. Chem. Soc. **2010**, 132, 14261–14272.
- (36) Cotton, F. A.; Wilkinson, G.; Murillo, C. A.; Bochmann, M. *Advanced Inorganic Chemistry*, 6th ed.; Wiley-Interscience: Hoboken, 1999.
- (37) Telser, J.; Pardi, L. A.; Krzystek, J.; Brunel, L. C. Inorg. Chem. 1998, 37, 5769-5775.
- (38) Dobe, C.; Andres, H. P.; Tregenna-Piggott, P. L. W.; Mossin, S.; Weihe, H.; Janssen, S. Chem. Phys. Lett. **2002**, 362, 387–396.
- (39) Dobe, C.; Noble, C.; Carver, G.; Tregenna-Piggott, P. L. W.; McIntyre, G. J.; Barra, A. L.; Neels, A.; Janssen, S.; Juranyi, F. *J. Am. Chem. Soc.* **2004**, *126*, 16639–16652.
- (40) Dobe, C.; Strassle, T.; Juranyi, F.; Tregenna-Piggott, P. L. W. *Inorg. Chem.* **2006**, *45*, 5066–5072.
- (41) Karunadasa, H. I.; Arquero, K. D.; Berben, L. A.; Long, J. R. Inorg. Chem. **2010**, 49, 4738–4740.
- (42) Krzystek, J.; Ozarowski, A.; Telser, J. Coord. Chem. Rev. 2006, 250, 2308-2324.
- (43) Barra, A. L.; Dossing, A.; Morsing, T.; Vibenholt, J. *Inorg. Chim. Acta* **2011**, 373, 266–269.

(44) Boynton, J. N.; Summerscales, O. T.; Grandjean, F.; Long, G. J.; Fettinger, J. C.; Power, P. P. Organometallics 2012, 31, 8556–8560.

- (45) Tarasov, V. F.; Shakurov, G. S.; Malkin, B. Z.; Ulanov, V. A. *Modern Applications of EPR/ESR*; Springer: Singapore, 1998.
- (46) König, E.; Schnakig, R.; Kanellakopulos, B.; Klenze, R. Chem. Phys. Lett. 1977, 50, 439-441.
- (47) Craig, G. A.; Murrie, M. Chem. Soc. Rev. 2015, 44, 2135-2147.
- (48) Neese, F.; Pantazis, D. A. Faraday Discuss. 2011, 148, 229-238.
- (49) Christou, G.; Gatteschi, D.; Hendrickson, D. N.; Sessoli, R. MRS Bull. **2000**, 25, 66–71.
- (50) Zadrozny, J. M.; Liu, J. J.; Piro, N. A.; Chang, C. J.; Hill, S.; Long, J. R. Chem. Commun. 2012, 48, 3927–3929.
- (51) Berry, J. F.; Cotton, F. A.; Murillo, C. A.; Chan, Z.-K.; Yeh, C.-W.; Chen, J.-D. In *Inorganic Syntheses*; Girolami, G. S., Sattelberger, A. P., Eds.; John Wiley & Sons, Inc.: Hoboken, 2014; Vol. 36, p 103.
- (52) Wang, J. F.; Wang, Z. X.; Clark, R. J.; Ozarowski, A.; van Tol, J.; Dalal, N. S. *Polyhedron* **2011**, *30*, 3058–3061.
- (53) Cornia, A.; Rigamonti, L.; Boccedi, S.; Clerac, R.; Rouzieres, M.; Sorace, L. Chem. Commun. **2014**, 50, 15191–15194.
- (54) Ye, S. F.; Neese, F. J. Chem. Theory Comput. 2012, 8, 2344-2351
- (55) Desrochers, P. J.; Telser, J.; Zvyagin, S. A.; Ozarowski, A.; Krzystek, J.; Vicic, D. A. Inorg. Chem. 2006, 45, 8930–8941.
- (56) Zadrozny, J. M.; Telser, J.; Long, J. R. Polyhedron 2013, 64, 209-217.
- (57) Stavretis, S. E.; Atanasov, M.; Podlesnyak, A. A.; Hunter, S. C.; Neese, F.; Xue, Z. L. *Inorg. Chem.* **2015**, *54*, 9790–9801.
- (58) Suturina, E. A.; Maganas, D.; Bill, E.; Atanasov, M.; Neese, F. *Inorg. Chem.* **2015**, *54*, 9948–9961.
- (59) Bill, E. *julX*; Max Planck Institute for Chemical Energy Conversion: Muelheim an der Ruhr.
- (60) Bain, G. A.; Berry, J. F. J. Chem. Educ. 2008, 85, 532-536.
- (61) van Tol, J.; Brunel, L. C.; Wylde, R. J. Rev. Sci. Instrum. 2005, 76, 074101.
- (62) Morley, G. W.; Brunel, L. C.; van Tol, J. Rev. Sci. Instrum. 2008, 79, 064703.
- (63) Krzystek, J.; Sienkiewicz, A.; Pardi, L.; Brunel, L. C. *J. Magn. Reson.* 1997, 125, 207–211.
- (64) Krzystek, J.; Zvyagin, S. A.; Ozarowski, A.; Trofimenko, S.; Telser, J. J. Magn. Reson. 2006, 178, 174–183.
- (65) Abragam, A.; Bleaney, B. Electron Paramagnetic Resonance of Transition Ions; Oxford Press: Oxford, 1970.
- (66) Boskovic, C.; Brechin, E. K.; Streib, W. E.; Folting, K.; Bollinger, J. C.; Hendrickson, D. N.; Christou, G. J. Am. Chem. Soc. 2002, 124,
- (67) Mishra, A.; Wernsdorfer, W.; Abboud, K. A.; Christou, G. J. Am. Chem. Soc. **2004**, 126, 15648–15649.
- (68) Milios, C. J.; Vinslava, A.; Wernsdorfer, W.; Moggach, S.; Parsons, S.; Perlepes, S. P.; Christou, G.; Brechin, E. K. J. Am. Chem. Soc. 2007, 129, 2754–2755.
- (69) AlDamen, M. A.; Clemente-Juan, J. M.; Coronado, E.; Marti-Gastaldo, C.; Gaita-Arino, A. J. Am. Chem. Soc. 2008, 130, 8874.
- (70) Lampropoulos, C.; Murugesu, M.; Harter, A. G.; Wernsdofer, W.; Hill, S.; Dalal, N. S.; Reyes, A. P.; Kuhns, P. L.; Abboud, K. A.; Christou, G. *Inorg. Chem.* **2013**, *52*, 258–272.
- (71) While the observed hysteresis is likely due to single-molecule magnet behavior of 2 and 3, it could also possibly be due to a phonon bottleneck where the magnitude of the |D| value is not relevant. This effect has been observed before in a metal—metal bonded dimer, but with hysteresis temperatures far below those observed here. See: Chen, L.; Ramsey, C. M.; Dalal, N. S.; Ren, T.; Cotton, F. A.; Wernsdorfer, W.; Chiorescu, I. *Appl. Phys. Lett.* 2006, 89, 252502.
- (72) Weil, J.; Bolton, J. R. Electron Paramagnetic Resonance Elementary Theory and Practical Applications, 2nd ed.; Wiley-Interscience: Hoboken, 2007.
- (73) Samuel, P. P.; Mondal, K. C.; Sk, N. A.; Roesky, H. W.; Carl, E.; Neufeld, R.; Stalke, D.; Demeshko, S.; Meyer, F.; Ungur, L.; Chibotaru, L. F.; Christian, J.; Ramachandran, V.; van Tol, J.; Dalal, N. S. J. Am. Chem. Soc. 2014, 136, 11964—11971.

(74) Montali, M.; Credi, A.; Prodi, L.; Gandolfini, T. M. Handbook of Photochemistry, 3rd ed.; CRC Press: New York, 2006.